Egypt. J. Chem. **Vol. 66**, No. SI: 13 pp. 167 - 185 (2023)

Egyptian Journal of Chemistry

http://ejchem.journals.ekb.eg/

Discovery and Synthesis of Novel Bio-Isostere of Purine Analogues Inhibiting SARS-CoV-2

Reham A. Mohamed-Ezzat,[a*] and Galal H. Elgemeie[b]

[a]*Chemistry of Natural & Microbial Products Department, Pharmaceutical and Drug Industries Research Institute, National Research Center, Cairo, 12622,Egypt*

[b]*Department of Chemistry, Faculty of Science, Helwan University, Cairo,11795, Egypt*

Abstract

The novel SARS-CoV2 (2019-nCoV) virus that causes COVID-19 is resistant to the current antiviral medications, leading to an extremely high fatality rate. The pathogen SARS-CoV2 is extremely infectious. Millions of people have been affected by COVID-19 worldwide, and the number is dangerously rising due to the ongoing rise in cases. Toward developing SARS-COV-2 inhibitors, many pyrimidine and purine analogs have been depicted. Thus in order to developing new purine analogs the synthetic approach to prepare methylsulfanylpyrimidine nuclei is accomplished. Successful generation of a new series of triazolopyrimidines (**TZP**) as a new bio-isostere purine analog is furnished under mild conditions with high yields in a different manner from the traditional approaches and avoided the sophisticated methods. The crosspondingtriazolopyrazolopyrimidines which are characterized by the presence of tri-fused heterocyclic ring system were also produced. Selected compounds were tested for inhibition of SARS-CoV-2 viral replication. The antiproliferativeefficacy of the newly synthesized compounds was also examined on a panel of NCI 60 human cancer cell lines. Our results demonstrated that the triazolopyrimidine**9b** is a very promising novel purine analog that focus and highlights the potential of the TPZ scaffold as anti-CoV agent and is worthy of further evaluation as a potential therapeutic agent.

Keywords: SARS-CoV2; COVID-19; anti-proliferative activity; purine analogs; *N*-cyanodithioiminocarbonate; triazolopyrimidines.

1.Introduction

Novel viruses pose a serious concern to humans because they have the propensity to spread quickly and cause major disease. Numerous viral disease epidemics have occurred over the past few decades, including those caused by Zika, Ebola, Nipah, HIN1, H7N9 Avian Influenza, SARS-CoV1, MERS-CoV [1] and recently the infection with the severe acute respiratory syndrome coronavirus 2 (SARS-CoV2) which causes the disease known as ‘‘coronavirus disease-19” (COVID-19) [2] which results in acute respiratory distress syndrome (ARDS) leading to respiratory distress, lung injury. The highly contagious disease‘s nature, the advent of novel, hyperinfective strains, and the restricted

*Corresponding author e-mail: reham_amgad_2010@yahoo.com;ra.mohamed-ezzat@nrc.sci.eg (R.A.Mohamed-Ezzat).
EJCHEM use only: Received date 04 March 2023; revised date 20 April 2023; accepted date 01 May 2023
DOI: 10.21608/EJCHEM.2023.196504.7681

availability of efficient, targeted medications are all serious causes for concern [3]. COVID-19 is classified as pandemic emergency by the World Health Organization, as the unique SARS-CoV2 infectious disease is dispersing quickly over the world. From mild to severe life threatening variants, COVID-19 symptoms can range in intensity [4]. As new corona viral variations evolve more quickly than anticipated, new corona viral strains are more lethal than older ones [5, 6]. Since its most recent outbreak, COVID-19 disease, often known as severe pneumonia, has spread around the world. There is currently no definite treatment for the COVID-19 disease. However, it appears that a key factor in determining the clinical efficacy of the various classes of medications is the time of their administration [7, 8]. Drugs that have been repurposed for the COVID-19 pandemic are commercially accessible, but it takes a lot of time and effort to assess their safety and effectiveness. Several pharmaceutical excipients have been shown to have antiviral activity in recent years, making them potential candidates for use against SARS-CoV-2 [9]. Therefore, developing broad-spectrum anti-viral molecules for a quick response is crucial for both bioweapon defences and dealing with outbreak crises [10]. Many drug candidats (Fig.1) which may inhibit infection and replication of SARS-CoV-2 were reported [11].Developing literature emphasized the utility of triazolopyrimidine (TZP) heterocycles in developing antiviral agents, with several compounds that indicated antiviral potencies against various DNA and RNA viruses. TZP core exemplifies a privileged structure for accomplishing biologically potent molecules, thanks to its advantageous pharmacokinetic features, the ability of TZP scaffold to launch multiple interactions with the molecular target, and the synthetic feasibility that consents to the different functionalization of the TZPs [12]. Numerous triazolopyrimidine (TP) compounds were reported for antiviral potencies against RNA polymerase of HCV, HIV, & influenza viruses that indicated vast pharmacological significance. These studies validate that TP analogs signify lead molecules for designing an active inhibitor in order to control the replication of virus. These inhibitors are considered as appropriate drug candidates against SARS-CoV-2 [13, 14]. The triazolopyrimidine core signifies one of the privileged scaffold in chemistry. Optimization of its synthetic approaches such as [3 + 2] cycloaddition reaction, aza-Wittig reaction, oxidation of aminopyrimidine Schiff bases, and condensation with 1,3-dicarbonyl substrates have been carried out to yield targeted triazolopyrimidines. The triazolopyrimidine ring has been comprehensively utilized as a model in medicinal chemistry for its assorted pharmacological features. Diverse medicinally potent molecules retaining triazolopyrimidine core, emphasizing the importance of this nucleus. The distinctive triazolopyrimidine scaffold displays an striking bioactive potential [15]. The [1,2,4]triazolo[1,5-*a*]pyrimidines involve a promising category of non-naturally occurring microtubule (MT)-active compounds. Aforementioned studies indicated that various triazolopyrimidine substitutions can generate molecules that either disrupt MT integrity or promote MT stabilization. These variances can have significant consequences in the therapeutic uses of triazolopyrimidines [16]. Additionally, there are inventions consider the importance of the

pyrazolopyrimidines as anti-viral agents further relates to bag pharmaceutical composition containing triazol-pyrimidine compound of novelty and these compounds for being used in treating respiratory syncytial virus infection [17,18].

In this research, we have designed and synthesized novel analogues comprising the TZP core in order to get additional SAR insights for this category of compounds and discover more potent drugs. It's worth noting that we have developed convenient methods for the regioselective synthesis of pyrimidine analogs to furnish novel class of *N*-substituted pyrimidines [19-22]. Also many analogs for nucleic acid components as the novel cytosine thioglycosideanalogs have been synthesized [23]. Additionally, many antiviral heterocyclic thioglycosides, such as pyrimidine thioglycosides [24, 25], which displayed a potent cytotoxic effect, and correspondingly we designated the dihydropyridinethioglycosides that are utilized as protein glycosylation's inhibitors [26, 27]. Additionally, several efficacious approaches for synthesizing modified nucleoside analogs have been accessed [28-30]. In biochemical reactions, these ring systems are remarkable as anti-metabolites [31, 32]. As part of our on-going research programme and among the strategies depicted to synthesize the purine and pyrimidine analogs, the current research emphases on synthesizing novel methylsulfanylpyrimidine, triazolopyrimidines (TZP) and their corresponding analogs. This synthesis is furnished via reacting dimethyl *N*-cyanodithioiminocarbonate with substituted acetohydrazides. Those analogs represent a number of novel purine analogues, which indicated a remarkable result toward Covid-19. Furthermore, in order to investigate the wide spectrum of this class of compounds, and as most of the anticancer agents were structural analogs of several purines, pyrimidines, and other essential metabolites and have developed as significant novel agents against several cancer types [33-35] the *in vitro* anti-proliferative activity of selected compounds was estimated.

2. Results and discussion

2.1 Synthesis

The substituted (1-arylethylideneamino)-1,6-di-hydropyrimidine-5-carbonitriles **5a-c** and the corresponding analogues **6a-c** were prepared through the step synthesis shown in scheme 1. The reaction of 2-cyano-N′-(1-arylethyl-idene)acetohydrazide (**1a-c**) with dimethyl N-cyanodithioiminocarbonate (**2**), as highly reactive intermediate [36, 37], in ethanol with anhydrous potassium hydroxide as the base furnished the substituted 1,6-dihydropyrimidine-5-carbonitrile respectively, in good yields.

The spectroscopic data's display of compounds **5** results are consistent with the proposed targeted structures. For further unambiguous proof of the structure of compound **5a**, its crystal structure was furnished upon crystallization to get the single crystal structure suitable to be measured. The X-ray investigation approves the existence of the substituted-(1-phenylethylideneamino)-1,6-dihydro-pyrimidine-5-carbonitrile form **5a** in solid state (Fig. 2) [38]. Compound **5** is furnished via from the reacting of **1** with **2,** the reaction is progressed through Michael reaction of the active methylene of **1** to the double bond in **2**, then cyclization of the formed adducts was occurred via methanethiol elimination and the addition to the –CN group. These latter compounds were transformed utilizing hydrazine hydrate into the corresponding

substituted pyrazolo [4,3-*e*]-1,2,4-triazolo[1,5-*a*] pyrimidine**6a-c** (Scheme 1).

In order to discover this approach 's scope and to establish whether the reaction of dimethyl *N*-cyanodithioiminocarbonate with 2-cyano-N′-(1-arylethylidene)acetohydrazide could be comprehensive to afford a general approach to ((*E*)-2-amino-4-methylsulfanyl-6-oxo-1-(1-arylethyl-idene-amino)-1,6-dihydropyrimidine-5-carbonitrile, we studied the reaction of dimethyl *N*-cyanodithioiminocarbonate**2** with other derivatives of the arylethylideneacetohydrazide. Interestingly, it has been found that the methoxy and methyl substitution of arylethyl-ideneacetohydrazidecyanoacetohydrazide reacts with **2** in the same condition as mentioned to produce the 2-amino-4-methylsulfanyl-6-oxo-1-(1-arylethylidene-amino)-1,6-dihydropyrimidine-5-carbonitrile but novel fused heterocyclic ring system, substituted tolyl- or- methoxyphenyl-[1,2,4]triazolo[1,5-*a*]pyrimidine-6-carbonitrile, is generated spontaneously as a result of intra-molecular ring closure to afford the substituted triazolo[1,5-*a*]pyrimidine-6-carbonitrile **9**. The mechanism is suggested to occur through oxidation of the methyl group to an aldehydic group, followed by elimination of formaldehyde [39] as shown in scheme 2. The ^{1}H NMR spectrum of compound **9b** revealed a singlet signal at δ 2.50 ppm for the protons of the SCH_3 group, a singlet signal at δ 3.82 ppm for the protons of the methoxy group, and the four aromatic protons appeared at the δ 7.02-7.86 ppm. The ^{1}H NMR also reveals the disappearance of the methyl proton which confirm the intra-molecular cyclization to form the triazolo [1,5-*a*] pyrimidine derivative. In a further experiment, compounds **9** is allowed to react with hydrazine hydrate under reflux to afford the corresponding analogs,the substituted pyrazolo [4,3-*e*]-1,2,4-triazolo[1,5-*a*] pyrimidine, **10** as accomplished in scheme 2. The individual structure of compounds **10** was established based on the elemental analysis and the spectral data. In additional experiments, 2-cyano-*N'*-(1-(pyridin-2-yl)ethylidene)acetohydrazide is used to produce the novel substituted (1-(pyridin-2-yl)ethylideneaminopyrimidine-5-carbonitrile **12**according to scheme 3. The X-ray analysis confirms the structure of the compoundin solid state (Fig. 3) [38]. Compound **12** was then reacted with hydrazine hydrate under reflux to furnish compound **13**.

Remarkably, some of the synthesized compounds revealed fluorescence features which prompted us to investigate its photo-physical properties. The photophysical properties of **9a**&**9b** are indicated. The absorption spectra of the compounds **9a**, **9b** were examined in DMSO. It can be clearly detected that the absorption spectrum of **9b** displayed a strong absorption band at 363 nm with other two weak absorption bands at 339 and 332 nm. Similar observations were recorded for the other derivative **9a** which reveals absorption band at 320 nm.

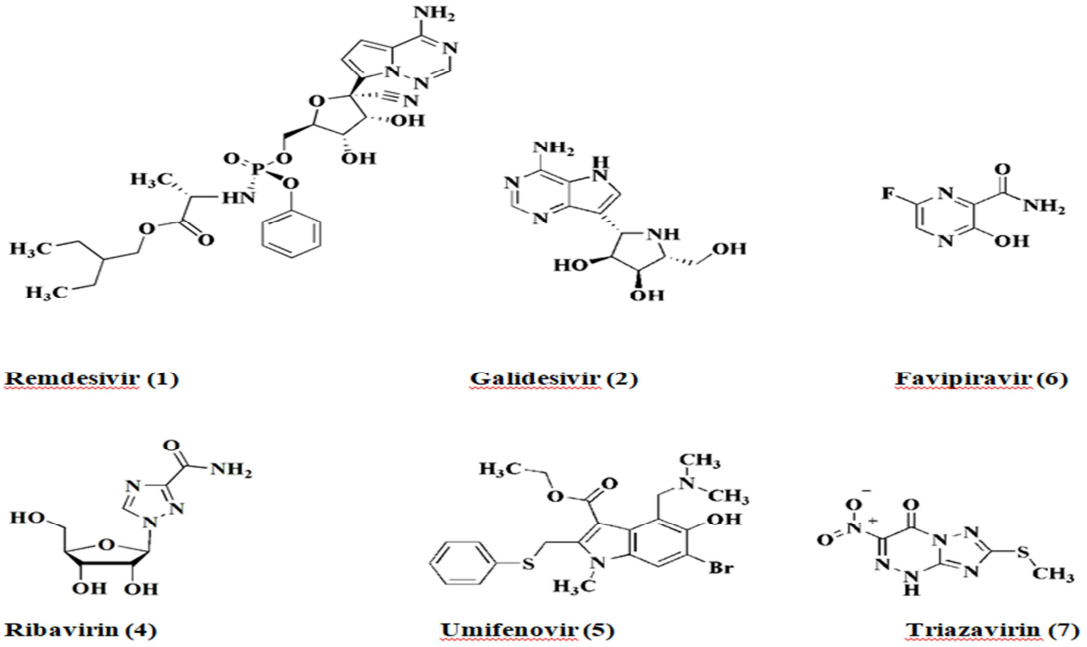

Figure 1: Candidate drugs against SARS-CoV-2 and COVID-19

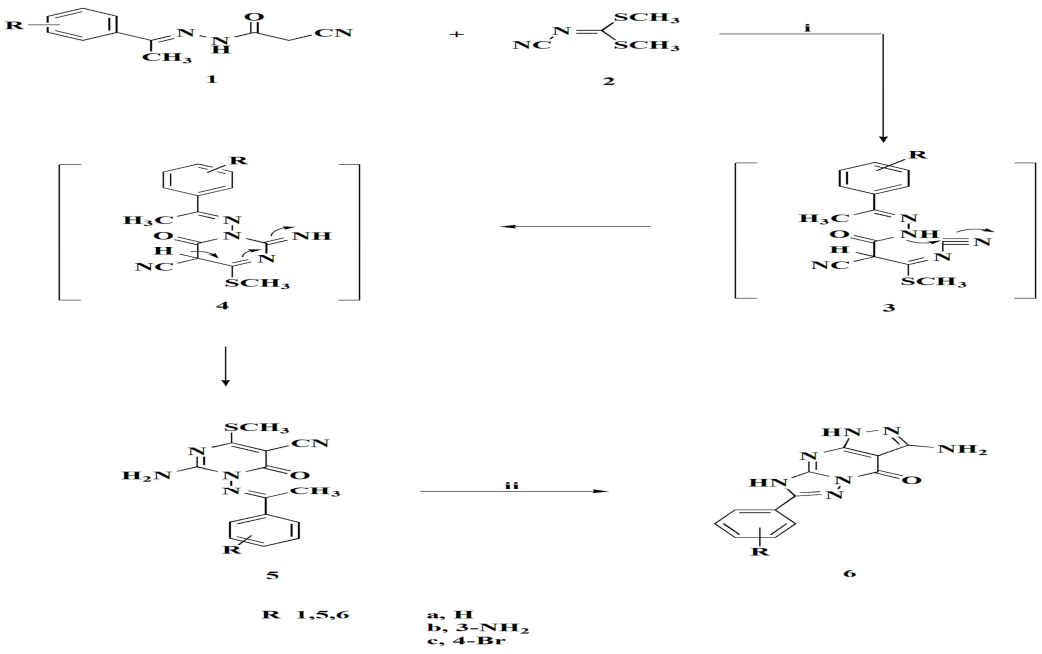

Reagents and conditions: i) Potassium hydroxide, EtOH, reflux, 3h. **ii)** Hydrazine hydrate, reflux, 3h

Scheme 1: Synthesis of Pyrazolopyrimidines as bio-isostere purine analogs

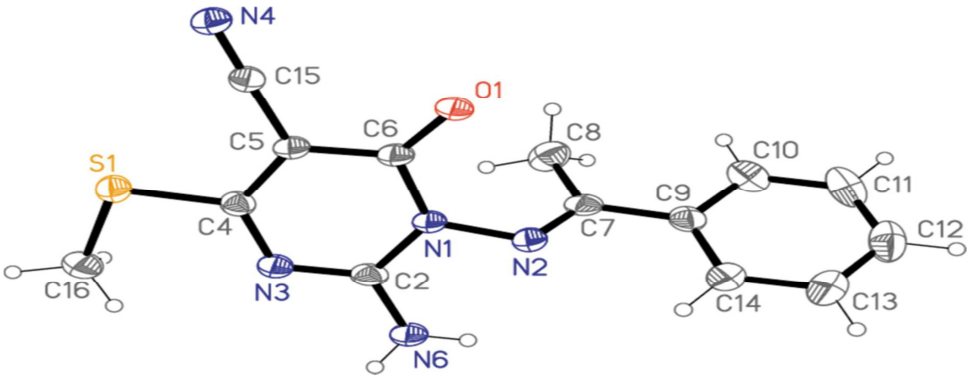

Figure 2: The structure of compound **5a** in the crystal. Ellipsoids correspond to levels of 50% probability. "Reproduced with permission of the International Union of Crystallography under the open-access licence" [38]

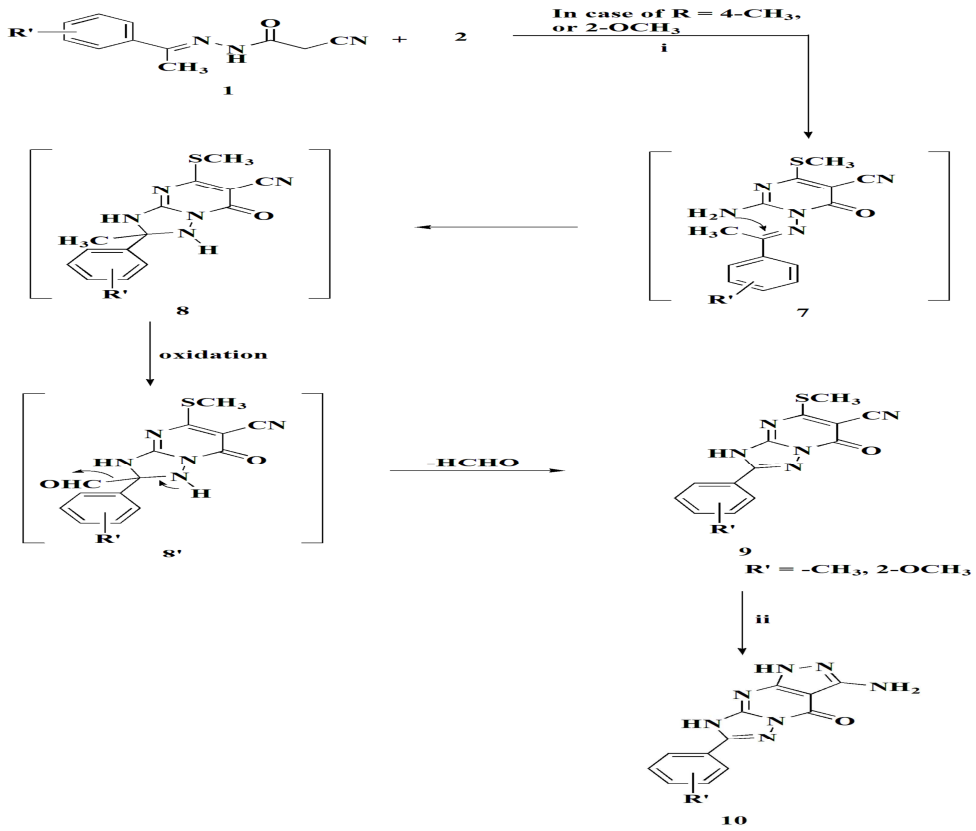

Reagents and conditions: i) Potassium hydroxide, EtOH, reflux, 3h. **ii)** Hydrazine hydrate, reflux, 3h

Scheme 2: Synthesis of Triazolopyrimidines as bio-isostere purine analogs

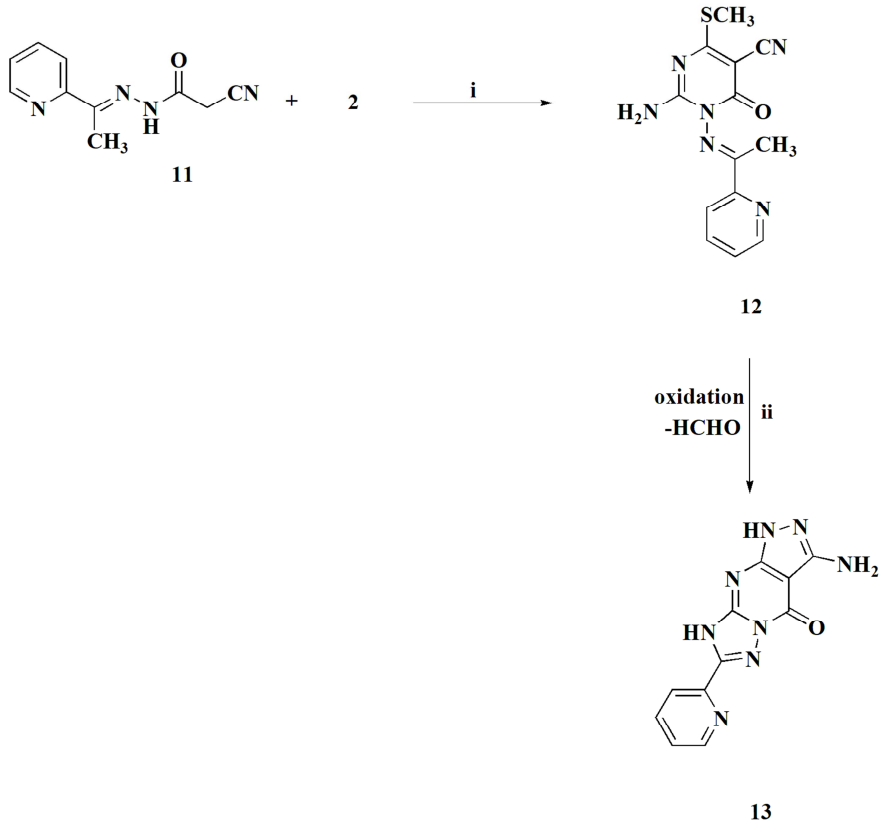

Reagents and conditions: i) Potassium hydroxide, EtOH, reflux, 30 min. **ii)** Hydrazine hydrate, reflux, 2h

Scheme 3: Synthesis of Pyrazolopyrimidines as bio-isostere purine analogs

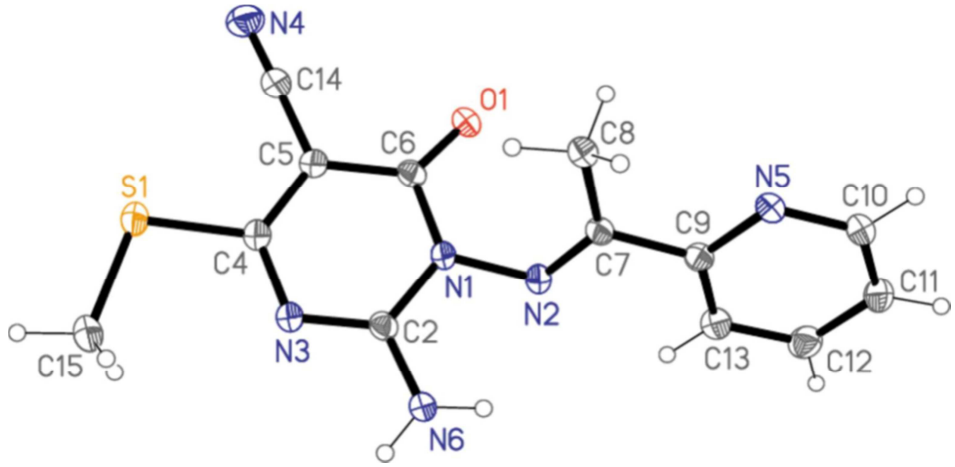

Figure 3: The structure of compound **12** in the crystal. Ellipsoids correspond to levels of 50% probability
"Reproduced with permission of the International Union of Crystallography under the open-access licence".[38]

Table 1

Determination of the Antiviral CC_{50} and IC_{50} of compounds (**5a–c**, **6a-b**, **9b**, **10b** and **12**) against SARS-COV-2 virus

Compound no.	CC_{50} (µmol)	IC_{50}(µmol)
5a	348.5	36.97
5b	2.151e+007	1969
5c	290.1	24.93
6a	59.04	0.0
6b	584.5	36.21
9b	2.151e+007	20.27
10b	582.4	443.9
12	280.5	22.33

Table 2

Antitumor properties of the compounds at a dose of 10 µM using human tumor cell lines

Panel/Cell line	**5a**	**5b**	**5c**	**6a**	**6b**	**9b**	**12**
Leukemia							
CCRF-CEM	101.39	97.45	94.86	97.69	99.31	98.35	94.39
HL-60(TB)	89.81	81.75	81.43	94.80	93.07	104.21	85.14
K-562	92.95	116.94	96.92	101.34	104.52	112.30	97.67
MOLT-4	99.01	102.86	94.43	106.22	101.73	100.89	90.66
RPMI-8226	109.99	105.28	102.66	101.63	104.35	104.12	104.36
SR	86.92	92.37	83.79	106.41	102.19	95.00	87.78
Non-Small cell Lung cancer							
A549/ATCC	92.15	102.76	105.87	99.95	105.46	93.86	92.52
EKVX	96.51	96.06	97.13	99.44	100.52	93.72	98.32
HOP-62	95.51	98.01	102.77	99.07	114.16	97.55	98.99
HOP-92	96.89	100.99	112.54	112.05	105.41	94.50	114.25
NCI-H226	98.10	99.73	103.46	106.67	104.57	99.26	103.52
NCI-H322M	105.35	97.10	93.39	92.61	93.15	95.21	94.79
NCI-H460	105.16	107.02	103.87	110.50	108.87	106.95	106.37
NCI-H522	96.64	103.98	97.03	100.13	102.12	104.04	101.63
Colon cancer							
COLO 205	125.45	115.25	124.58	108.90	114.20	107.93	113.27
HCC-2998	110.80	110.09	103.38	105.49	114.07	104.45	105.00
HCT-116	90.49	107.09	95.79	94.90	99.96	105.35	89.55

HCT-15	101.95	105.83	94.42	97.55	102.93	100.46	99.25
HT29	112.76	106.52	107.82	110.40	118.29	117.34	106.91
KM12	105.43	116.08	106.55	104.93	108.97	108.93	107.58
SW-620	100.55	105.15	101.20	103.17	105.63	99.34	103.66
CNS Cancer							
SF-268	118.74	109.93	112.33	109.00	106.70	111.17	106.40
SF-295	96.99	98.42	93.37	96.70	101.73	100.04	100.72
SF-539	97.53	98.74	104.95	97.32	100.06	101.38	98.22
SNB-19	96.73	94.64	99.81	95.23	98.26	95.88	98.30
SNB-75	107.79	100.34	113.66	124.97	117.42	101.94	118.92
U251	92.54	120.72	98.32	112.71	109.07	107.82	98.57
Melanoma							
MALME-3M	105.21	102.65	112.81	102.42	105.23	99.84	105.81
M14	103.47	102.05	107.32	99.32	108.33	104.17	96.04
MDA-MB-435	106.52	108.36	97.42	110.40	105.71	110.83	113.35
SK-MEL-2	110.75	113.41	112.67	115.13	114.30	114.45	115.96
SK-MEL-28	106.14	102.74	100.57	109.76	113.77	117.18	111.63
SK-MEL-5	101.40	100.22	98.99	100.64	99.92	101.09	100.73
UACC-257	103.89	113.98	109.92	105.80	115.61	112.16	92.90
UACC-62	101.06	101.38	94.46	98.38	100.69	99.91	99.40
Ovarian cancer							
IGROV1	105.07	98.30	110.10	102.35	103.65	101.48	114.12
OVCAR-3	118.89	121.08	118.75	118.92	115.80	118.26	117.61
OVCAR-4	114.41	106.82	110.72	114.29	111.43	118.41	116.78
OVCAR-5	106.40	98.85	103.43	109.21	113.90	110.11	106.63
OVCAR-8	97.81	105.16	102.70	107.52	106.18	96.94	101.39
NCI/ADR-RES	114.63	104.79	102.41	108.73	104.83	102.18	104.30
SK-OV-3	137.64	126.59	109.03	104.62	123.60	145.21	115.77
Renal Cancer							
786-0	108.92	101.98	96.80	104.72	108.56	103.04	91.45
ACHN	109.21	106.61	105.63	100.89	108.58	105.53	108.49
CAKI-1	96.74	98.70	104.54	102.60	99.57	91.78	101.54
RXF 393	122.28	110.59	116.71	117.95	116.82	121.48	118.06
SN12C	99.37	99.79	98.07	101.26	101.29	100.95	100.73

TK-10	124.35	109.04	116.80	124.45	119.90	179.03	120.38
UO-31	95.74	84.64	92.09	92.81	94.59	79.55	97.69
Prostate Cancer							
PC-3	98.47	92.61	104.11	97.08	97.05	93.17	97.63
DU-145	108.71	108.45	106.11	111.28	112.59	112.85	109.48
Breast Cancer							
MCF7	88.29	94.54	88.89	91.95	92.98	86.74	93.66
MDA-MB-231/ATCC	105.65	101.00	110.58	104.87	109.76	99.01	103.91
HS 578T	107.92	108.47	119.22	103.88	115.75	106.58	108.17
BT-549	106.70	99.14	101.20	112.19	107.99	112.33	91.99
T-47D	102.04	96.96	93.84	114.55	103.60	99.94	118.64
MDA-MB-468	98.13	98.40	107.26	106.23	98.74	104.98	103.43

3. Antiviral Activity

3.1. SARS-COV-2. A series of the novel synthesized targeted compounds were screened to evaluate the antiviral activity against SARS-COV-2 virus for the estimation of the half-maximal cytotoxic concentration (CC_{50}) and inhibitory concentration 50 (IC_{50}), (Table 1 & Fig 4). The MTT assay's results showed that some compounds possess potent and remarkable potency against SARS-CoV-2.

Compound **9b** was the most safe compounds on the cells and had anti-viral activity against SARS-CoV-2 IC_{50}=20.27.

Compounds have slight antiviral activity were **12, 5c, 6b, 5a** IC_{50}= 22.3, 24.93, 36.2 and 36.9 µmolrespectivily. The compounds had low antiviral activity were **5b**&**10b**, IC_{50}=1969, and 443.9µmol respectivily but Compound **6a** not revealed any activity. Thus, the current research affirmed the potencies of some of the estimated compounds particularly **9b** as potent COVID-19's inhibitor.

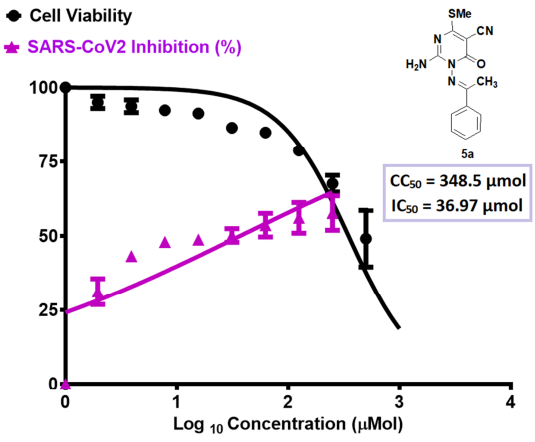

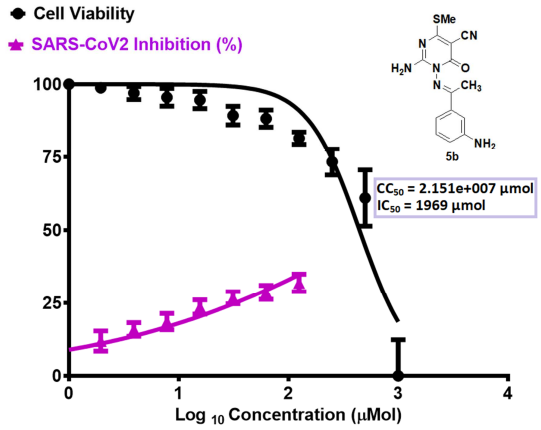
Cell Viability
SARS-CoV2 Inhibition (%)
5b
CC50 = 2.151e+007 µmol
IC50 = 1969 µmol
Log 10 Concentration (µMol)

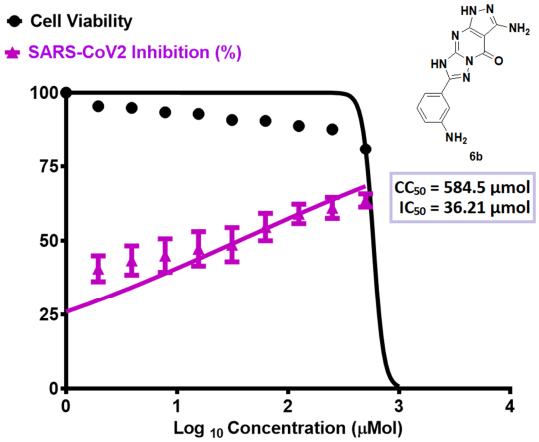
Cell Viability
SARS-CoV2 Inhibition (%)
6b
CC50 = 584.5 µmol
IC50 = 36.21 µmol
Log 10 Concentration (µMol)

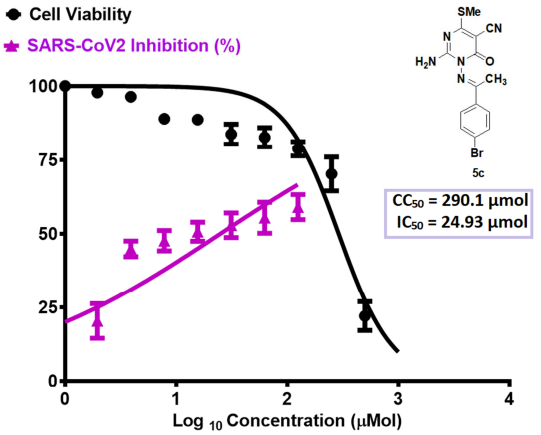
Cell Viability
SARS-CoV2 Inhibition (%)
5c
CC50 = 290.1 µmol
IC50 = 24.93 µmol
Log 10 Concentration (µMol)

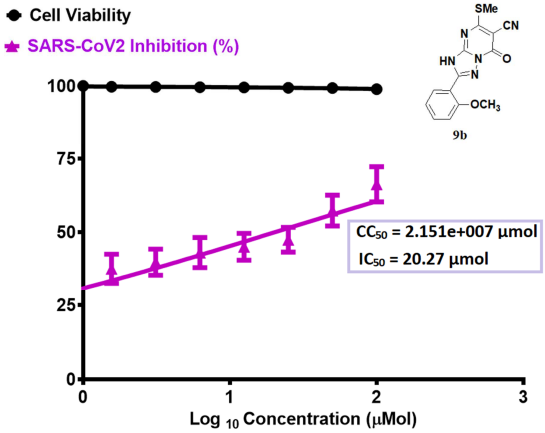
Cell Viability
SARS-CoV2 Inhibition (%)
9b
CC50 = 2.151e+007 µmol
IC50 = 20.27 µmol
Log 10 Concentration (µMol)

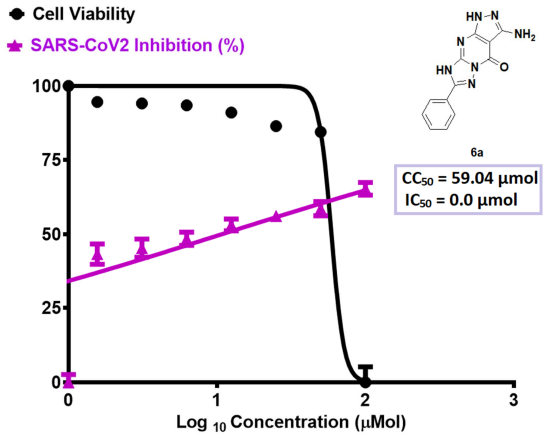
Cell Viability
SARS-CoV2 Inhibition (%)
6a
CC50 = 59.04 µmol
IC50 = 0.0 µmol
Log 10 Concentration (µMol)

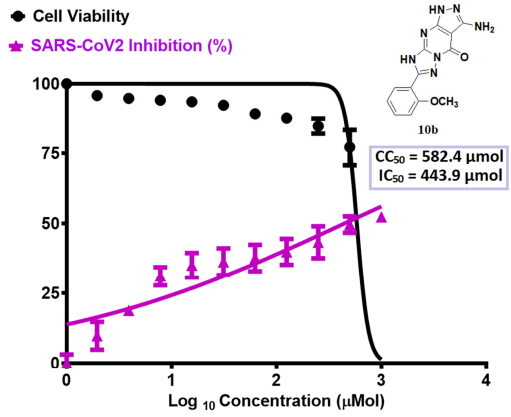
Cell Viability
SARS-CoV2 Inhibition (%)
10b
CC50 = 582.4 µmol
IC50 = 443.9 µmol
Log 10 Concentration (µMol)

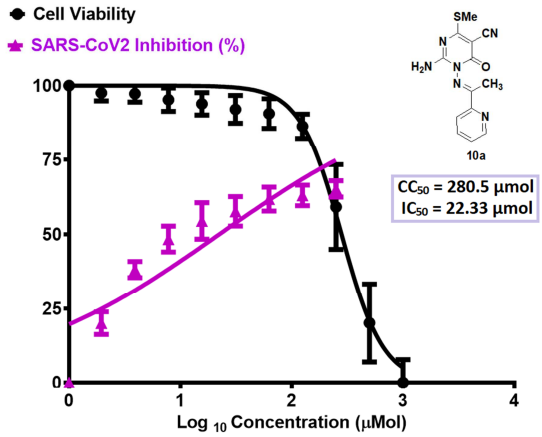

Figure 4: Graphs of the cytotoxicity concentration 50 (CC_{50}) of compounds (**5a–c**, **6a-b**, **9b, 10b** and **12**): on Vero E6 cells

4. *In-vitro* Anti-proliferative activity

The *in vitro* anti-proliferative activity against NCI 60-cell line panel was estimated.Most of the targeted structures have been selected via the National Cancer Institute "NCI", NIH, USA through the Developmental Therapeutic Program (DTP). The process of screening employs various human tumor cell lines, expressive melanoma, leukemia, brain, lung, ovary, colon, kidney, prostate & breast cancers.

According to computer-aided design, compounds having drug-like modes of action are given priority in the service of the NCI screening.

The submitted compounds are chosen for screening based on their capacity to diversify the NCI small molecule compound collection.

The compounds which have been selected were coded with the respective NCI codes NSC D-832394, NSC D-832400, NSC D-832396, NSC D-832397, NSC D-832398, NSC D-832393 & NSC D-832395 representing the various structures of this study, were examined on the NCI cell panel. The consequences are stated as cell growth percent for every compound on each of the NCI cell line.

Compounds **9b**, **5b**,and **5c** displayed the highest potency as compared to the rest of the synthesized compounds, in a descending order, in the *in-vitro* screening on the cell lines. Compounds **5a** & **12** revealed moderate activities in the *in vitro* screening on some of the tested cell lines, while compounds **6a & 6b** exhibited low potency (Table 2).

Compound **9b** the most potent among the tested compounds,showed remarkably lowest cell growth promotion against renal cancer UO-31 cell line (GP = 79.55%). Compound **5b** was moderately active on leukemia HL-60(TB) cell line (GP = 81.75%), and renal cancer UO-31 cell line (GP = 84.64%). Compound **5c** was moderately active on leukemia SR cell line (GP = 83.79%). Compound **5a** displayed moderate activity on theleukemia SR cell line (GP = 86.92%).

Of note that compound **10** was moderately active on leukemia HL-60(TB) cell line (GP = 85.14%). On the other hand, compounds **6a** & **6b** were moderately active on Breast Cancer MCF7 cell line with cell growth promotion of 91.95 & 92.98 respectively.

5. Structure–Activity Relationships

The antiviral activity of compounds **5a–c**, **6a–b**, **9b**, **10b** and **12** against SARS-COV-2 viruses was estimated as shown in table 1. Interestingly, the new substituted [1,2,4]triazolo[1,5-*a*]pyrimidine-6-carbonitrile (**9b**) verified significant increase in inhibiting SARS-COV-2 virus (IC_{50}=20.27) comparable to structures without this ring system.

On the other hand, the same compound, **9b**, with the fused heterocyclic ring system having a methoxy substituent at the phenyl group also effectively exhibited the greatest antiproliferative activity among the tested compounds, with lowest cell

growth promotion against renal cancer UO-31 cell line (GP = 79.55%), respectively, showing more activity against renal cancer as compared with the other cell lines (Fig. 5).

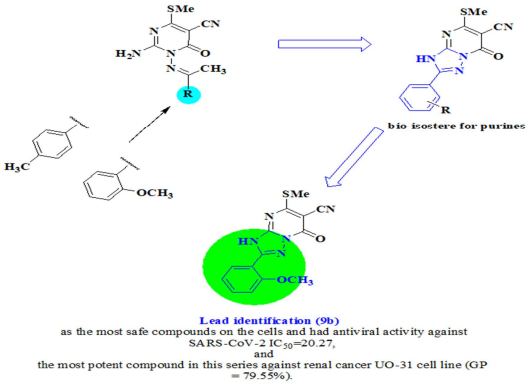

Figure 5: SAR of compound **9b**

6. Conclusions

For the search of novel therapeutic purine analog, we have accessed an efficient facile one-step synthesis of alkythiopyrimidineanalogs, pyrazolo[3,4-*d*]pyrimidines and TZP derivatives as anti-SARS CoV-2 compounds which have been accomplished using the highly reactive dimethyl *N*-cyanodithioiminocarbonate. Among the novel synthesized analogs, the triazolopyrimidine**9b** has the potential for anti-SARS-CoV-2 agents s' development. Remarkably, the TZP compound **9b** indicated anti-SARS-CoV2 activity with an IC_{50} value of 20.27 µM and was the most safe compound on the cells. The anti-proliferativeefficacy of selected synthesized compounds was also investigated on a panel of NCI 60 cancer cell lines. The TZP, **9b**, also effectively displayed the greatest anti-proliferative activity among the tested compounds, with lowest cell growth promotion against renal cancer UO-31 cell line (GP = 79.55%).

Conflict of interest

There is no conflict of interest.

7. Experimental

7.1 Chemical Methods. Monitoring the progress of the reaction was performed using TLC on the pre-coated silica gel 60 F_{245}aluminium plates using UV light for visualization. The melting point was uncorrected and was determined on a Stuart SMP30 apparatus. Spectroscopic determinations of the compounds were performed in faculty of pharmacy in the Drug Discovery, Research & Development Center at Ain Shams University, and National Research Centre Cairo, Egypt. TheNMR spectra were measured on Bruker Fourier 400 & 500 (at 400 MHz & 500 MHz, respectively) at 300 K. The Anti-SARS-COV-2 Virusbiological assays were performed at the Center of Scientific Excellence for Influenza Viruses, Environmental Research Division, National Research Center (NRC), Dokki, Cairo 12622, Egypt.

The antitumor screening was performed at the National Cancer Institute, Bethesda-Maryland, USA.

7.2 Synthesis & crystallization

7.2.1. General procedure for synthesizing compounds 5: A mixture of 2-cyano-*N*′-(1-aryl-ethylidene)acetohydrazide (**1**) (0.01 mol) and compound **2** (0.01 mol) was allowed to reflux in ethyl alcohol (10 mL) in the presence of anhydrous potassium hydroxide (0.01 mol). After pouring the mixture onto ice water; the formed product thus yielded was filtered and then re-crystallized using *dimethylformamide*.

7.2.1.1. 1-(1-phenylethylideneamino)-2-amino-1,6-dihydro-4-(methylthio)-6-oxopyrimidine-5-carbonitrile 5a Refluxingcompound (**1a**) with

compound **2** was carried out for 3 hours. Compound **5a** was yielded as a pale yellow solid (92%); m.p. 224-227 °C; IR (cm^{-1}) 3719 and 3437 (NH_2), 2202 (CN) and 1657 (C=O). ^{1}H-NMR (400 MHz, DMSO-d_6): 2.20 (s, 3H, CH_3), 2.55 (s, 3H, SCH_3), 8.52 (s, br, 2H, NH_2), 8.045–8.065 (d, J = 8Hz, 2H, 2CH), 7.59–7.62 (m, 1H, CH), 7.50–7.54 (m, 2H, 2CH). Anal.Calcd.for $C_{14}H_{13}N_5OS$ (299.35): C, 56.17; H, 4.38; N, 23.40; S, 10.71%. Found: C, 55.89; H, 4.25; N, 23.15; S, 10.52%.

7.2.1.2. 1-(1-(3-aminophenyl)ethylideneamino)-2-amino-1,6-dihydro-4-(methylthio)-6-oxopyrimidine-5-carbonitrile 5b According to general procedure, (*E*)-*N*'-(1-(3-aminophenyl)ethylidene)-2-cyanoacetohydrazide (**1b**) was allowed to reflux with compound **2** for 3 hours. Compound **5b** was yielded as buff solid (67%); mp 235-236 °C; IR (cm^{-1}) 3177, 3401 & 3325 (NH_2), 2210 (CN) and 1621 (C=O). ^{1}H-NMR (400 MHz, DMSO-d_6): 2.10 (s, 3H, CH_3), 2.54 (s, 3H, SCH_3), 5.28 (s, 2H, NH_2), 6.77–6.80 (m, 1H, CH), 7.14–7.15 (d, 2H, 2CH), 7.26 (s, 1H, CH), 8.48 (s, br, 1H, NH_2); Anal. Calcd.For.$C_{14}H_{14}N_6OS$ (314.37): C, 53.49; H, 4.49; N, 26.73; S, 10.20. Found: C, 53.49; H, 4.48; N, 26.72; S, 10.20.

7.2.1.3. 1-(1-(4-bromophenyl)ethylideneamino)-2-amino-1,6-dihydro-4-(methylthio)-6-oxopyrimidine-5-carbonitrile 5c According to general procedure, (*E*)-*N*'-(1-(4-bromophenyl)ethylidene)-2-cyanoacetohydrazide (**1c**) was allowed to reflux with compound **2** for three hours. Compound **5c** was yielded as a (70%) colorless crystals; mp 243-244 °C; IR (cm^{-1}) 3400 (NH_2), 2207 (CN) & 1648 (C=O). ^{1}H-NMR (400 MHz, DMSO-d_6): 2.26 (s, 3H, CH_3), 2.5 (s, 3H, SCH_3), 7.65-7.70 (m, 2H, 2CH), 7.84-7.87 (d, 2H, 2CH), 8.03-8.05 (d, 1H, NH); Anal. Calcd.For.$C_{14}H_{12}BrN_5OS$ (378.25): C, 44.46; H, 3.20; Br, 21.12; N, 18.52; S, 8.48. Found: C, 44.45; H, 3.20; Br, 21.12; N, 18.50; S, 8.48.

7.2.2. General procedure for synthesizing compounds 6:

The substituted methylsulfanylpyrimidine (**5**) (0.01 mol) was reacted with hydrazine hydrate (0.03 mol) at reflux for three hours. The precipitate is filtered off washed with ethyl alcohol, then re-crystallized from ethanol.

7.2.2.1. 3,7-dihydro-2-phenyl-7-oxo-pyrazolo [4,3-e]-1,2,4-triazolo[1,5-a]*pyrimidine *6a According to general procedure, Compound **6a** was afforded as a pale yellow solid (53%); mp 326 °C; ^{1}H-NMR (400 MHz, DMSO-d_6) δ 5.17 (s, 2H, NH_2), 7.35-7.38 (m, 1H, CH), 7.40-7.46 (d, 2H, CH), 10.81 (s, H, 1NH),11.30 (s, H, 1NH); Anal. Calcd.For.$C_{12}H_9N_7O$ (267.25): C, 53.93; H, 3.39; N, 36.69. Found: C, 53.93; H, 3.37; N, 36.67.

7.2.2.2. 3,7-dihydro-2-(3-aminophenyl)-7-oxo-pyrazolo [4,3-e]-1,2,4-triazolo[1,5-a]*pyrimidine *6b As described in general method, Compound **6b** was furnished as buff solid (61%); mp >340 °C; ^{1}H-NMR (400 MHz, DMSO-d_6) δ 5.10 (s, 2H, NH_2), 5.15 (s, 2H, NH_2), 6.97 (m, 2H, CH), 8.09 (d, 2H, CH), 11.26 (s, H, 1NH),11.45 (s, H, 1NH); Anal. Calcd.For.$C_{12}H_{10}N_8O$ (282.26): C, 51.06; H, 3.57; N, 39.70. Found: C, 51.05; H, 3.56; N, 39.68.

7.2.3. General procedure for synthesizing compounds 9: The substituted acetohydrazide (**1**) (0.01 mol) and compound **2** (0.01 mol) was allowed

to reflux in ethyl alcohol (10 mL) in the presence of anhydrous potassium hydroxide (0.01 mol). After pouring the mixture onto ice water; the precipitate thus yielded was then filtered and then re-crystallized using dimethylformamide.

7.2.3.1. 3,7-dihydro-5-(methylthio)-7-oxo-2-p-tolyl-[1,2,4]triazolo[1,5-a]pyrimidine-6-carbonitrile (9a)

According to general procedure, (E)-2-cyano-*N*'-(1-p-tolylethylidene)acetohydrazide was allowed to reflux with compound **2** for three hours . Compound **9a** was yielded as a buff solid (91%); mp 325-328 °C; ^{1}H-NMR (400 MHz, DMSO-d_6) δ 2.36 (s, 3H, CH_3), 2.50 (s, 3H, SCH_3), 7.29 (d, *J* = 8Hz, 2H, CH), 8.00 (d, *J* = 8Hz, 2H, CH); ^{13}C- NMR (400 MHz, DMSO-d_6): δ 13.08, 21.52, 78.92, 118.16, 126.93, 129.25, 129.71, 139.62, 156.74, 158.31, 161.71, 167.56.Anal.Calcd.For.$C_{14}H_{11}N_5OS$ (297.34): C, 56.55; H, 3.73; N, 23.55; S, 10.78. Found: C, 56.54; H, 3.72; N, 23.54; S, 10.76.

7.2.3.2. 3,7-dihydro-2-(2-methoxyphenyl)-5-(methylthio)-7-oxo-[1,2,4]triazolo[1,5-a]pyrimidine-6-carbonitrile (9b)

As described in the general procedure, (*E*)-2-cyano-*N*'-(1-(2-methoxyphenyl)ethylidene)acetohydrazide was allowed to reflux with **2** for three hours. Compound **9b** was yielded as a yellow crystal (93%); mp > 300 °C; ^{1}H-NMR (400 MHz, DMSO-d_6) δ 2.50 (s, 3H, SCH_3), 3.82 (s, 3H, OCH_3), 7.02-7.06 (t, 1H, CH), 7.13-7.16 (d, 1H, CH), 7.41 - 7.46 (t, 1H, CH), 7.83 - 7.86 (d, 1H, CH); Anal. Calcd.For.$C_{13}H_{11}N_7O_2$(297.27): C, 52.52; H, 3.73; N, 32.98. Found: C, 52.50; H, 3.72; N, 32.96.

7.2.4. General procedure for synthesizing compounds 10: The substituted methylsulfanylpyrimidine (**9**) (0.01 mol) was reacted with hydrazine hydrate (0.03 mol) at reflux for three hours. The solid product is filtered off and is washed with ethanol, then re-crystallized from ethanol.

***7.2.4.1. 3,7-dihydro-2-(p-tolyl)-7-oxo-pyrazolo [4,3-e]-1,2,4-triazolo[1,5-a]*pyrimidine(10a)**

According to general procedure, Compound **10a** was afforded as a grey solid (65%); mp > 360 °C; ^{1}H- NMR (400 MHz, DMSO-d_6) δ 2.36 (s, 3H, CH_3), 4.90 (s, 2H, NH_2), 7.92-8.00 (d, 2H, CH), 7.22-7.31 (d, 2H, CH); Anal. Calcd.For.$C_{13}H_{11}N_7O$ (281.27): C, 55.51; H, 3.94; N, 34.86. Found: C, 55.50; H, 3.93; N, 34.84.

7.2.4.2. 3,7-dihydro-2-(2-methoxyphenyl)-7-oxo-pyrazolo [4,3-e]-1,2,4-triazolo[1,5-a]pyrimidine (10b)

According to general procedure, Compound **10b** was furnished as buff solid (64%); mp 320 °C; ^{1}H-NMR (400 MHz, DMSO-d_6) δ 3.82 (s, 3H, OCH_3), 4.89 (s, 2H, NH_2), 7.02 (t, 1H, CH), 7.11 (d, *J* = 8Hz, 1H, CH), 7.38 (t, 1H, CH), 7.825 (d, *J* = 4Hz, 1H, CH), 10.77 (s, H, 1NH);^{13}C-NMR (400 MHz, DMSO-d_6): δ 8.01, 56.10, 88.32, 112.50, 120.51, 130.28, 131.46, 150.98, 155.11, 157.17, 157.82, 159.85. Anal.Calcd.For. $C_{13}H_{11}N_7O_2$ (297.27): C, 52.52; H, 3.73; N, 32.98. Found: C, 52.51; H, 3.71; N, 32.97.

7.2.5. General procedure for synthesizing compound 12: A mixture of compound **11** (0.01 mol) and compound **2** (0.01 mol) in the presence of potassium hydroxide anhydrous (0.01 mol) was allowed to reflux in ethyl alcohol (10 mL). After pouring the mixture onto ice water; the precipitate thus yielded was then filtered and re-crystallized using *dimethylformamide*.

7.2.5.1.1-(1-(pyridin-2-yl)ethylideneamino)-2-amino-1,6-dihydro-4-(methylthio)-6-oxopyrimidine-5-carbonitrile (12) Compound **11** was allowed to reflux with compound **2** for thirty minutes. Compound **12** was yielded as buff crystals (80%); m.p. 376-379 °C; IR (cm^{-1}) 3774 (NH_2), 2172 (CN) & 1635 (C=O). 1H-NMR (400 MHz, DMSO-d_6): 2.20 (s, 3H, CH_3), 2.51 (s, 3H, SCH_3), 8.54 (s, br, 2H, NH_2), 8.73–8.74 (d, J = 4Hz, 1H, CH), 8.29–8.31 (d, J = 8Hz, 1H, CH), 7.97 (t, 1H, CH); 7.61 (t, J = 8Hz, 1H, CH). Anal.Calcd.for $C_{13}H_{12}N_6OS$ (300.34): C, 51.99; H, 4.03; N, 27.98; S, 10.68. Found: C, 51.73; H, 4.22; N, 27.71; S, 10.39%.

7.2.6. General procedure for synthesizing compounds 13: The substituted methylsulfanylpyrimidine (**12**) (0.01 mol) was reacted with hydrazine hydrate (0.03 mol) at reflux for two hours. The solid product is filtered off and is washed with ethyl alcohol, then re-crystallized from ethanol.

7.2.6.1. 5-(1-(pyridin-2-yl)ethylideneamino)-3,6-diamino-1H-pyrazolo[3,4-d]pyrimidin-4(5H)-one (13)

According to general procedure, Compound **13** was afforded as a brown solid (50%); mp 312-314 °C; ^{1}H- NMR (400 MHz, DMSO-d_6) δ 5.16 (s, 2H, NH_2), 7.19 (m, 2H, CH), 8.11 (d, 1H, CH), 11.24 (s, H, 1NH),11.50 (s, H, 1NH); Anal. Calcd.For.$C_{11}H_8N_8O$ (268.23): C, 49.25; H, 3.01; N, 41.77. Found: C, 49.24; H, 3.00; N, 41.76.

7.4. Cytotoxicity Assay

7.5. SARS-COV2

7.5.1. MTT Cytotoxicity Assay

Stock solutions of the examined samples were set in DMSO (10%) in ddH_2O and then diluted to the employed solutions with the *DMEM* to determine the half maximum cytotoxic concentration (CC_{50}). The cytotoxic activity of the extracts was investigated in VERO-E6 cells by utilizing the 3-(4, 5-dimethylthiazol -2-yl)-2, 5-diphenyltetrazolium bromide (MTT) method with minor alterations. Concisely, the cells were seeded in 96-well plates (100 µl/well at a density of 3×10^5 cells/ml) and their incubation were performed for 24 hour in 5% carbon dioxide at 37 °C. Cells were given treatments in triplicates at varying doses of the investigated substances after 24 hours. Twenty four hour far ahead, the supernatant was cast-off, and cell mono-layers were then washed using sterile 1x phosphate buffered saline (PBS) three intervals successively and MTT solution (20 µl of 5 mg/ml stock solution) was added to each well and then incubated for 4 hours at thirty seven degree Celsius, then medium aspiration was followed. The formed formazan crystals were dissolved with 200 µl of acidified isopropyl alcohol (0.04 M hydrochloric acid in isopropyl alcohol = 0.073 ml hydrochloric acid in 50 ml isopropyl alcohol) in each well. Formazan solutions' absorbance was determined at λ max 540 nm with 620 nm utilizing a multiwall-plate reader. Calculating the concentration that displayed 50% cytotoxicity (CC_{50}) was done using a plot of % cytotoxicity versus sample concentration.

7.6. Estimation of the inhibitory Concentration 50 % (IC_{50})

2.4×10^4 Vero E6 cells were spread onto tissue culture plates (96-well) and then treated for an entire night at 37°C with 5% carbon dioxide.

The virus, hCoV-19/Egypt/NRC-03/2020 (Accession No. on GSAID/ EPI ISL 430820), was then applied to the cell monolayers and left on them for an additional hour at room temperature.

Thereafter, DMEM (100µl) containing various test drug concentrations was applied on top of the cell monolayers.

The cells were then fixed with 4% polyoxymethylene (100µl) for twenty minutes, stained with crystal violet (0.1%) in distilled water at room temperature for fifteen minutes, and then incubated in a 5% carbon dioxide incubator at thirty seven degree Celsius for the following 72 hours. Staining of the cells was carried out with crystal violet (0.1%) in DH_2O at room temperature for 15 minutes after being fixed with 4% polyoxymethylene(100 µl) for 20 minutes. The color's optical density was then measured at 570 nm utilizing an AnthosZenyth 200rt-plate reader after the crystal violet dye had been dissolved utilizing methyl alcohol (100 µl) each well (AnthosLabtec Instruments, Heerhugowaard, Netherlands). The IC_{50} of a compound is the amount needed to be reduced by 50% the viral-induced cytopathic effect (CPE) in comparison to virus control.

3.7. *In vitro* Anti-proliferative activity

Primary anticancer assays were carried out as referred to the NCI's protocol [40-44]. The compounds were added at single concentration and the cell culture was then incubation is performed for forty eight hours. Sulforhodamine B (SRB), a protein binding dye, was utilized to identify the endpoints (SRB). The compound's results are expressed as percent growth (GP%) of the treated cells comparable to the untreated cells related to control (Figure 3). Range of growth (%) indicated the highest & the lowest growth that originated for several cancer cell lines with concern to the sensitivity against the individual cell lines at the primary single high dose (10^{-5}M).

Acknowledgments

We would like to thank the National Cancer Institute, Bethesda-Maryland, USA for performing the antitumor screening.

- The study was approved under number 17444052023by theMedical Research Ethics Committee(MERC)fedral (accurance no. : FWA 00014747).

References

[1] D. Guo, Old weapon for new enemy: Drug repurposing for treatment of newly emerging viral diseases, Virol Sin. 35 (2020) 253-255. https://doi.org/10.1007/s12250-020-00204-7.
[2] Y. Chen, L. Li, SARS-CoV-2: Virus dynamics and host response, Lancet Infect Dis. 20 (2020) 515-516. https://doi.org/10.1016/S1473-3099(20)30235-8.
[3] S. Kumar, B. Singh, P. Kumari, P.V. Kumar, G. Agnihotri, S. Khan, T. Kant Beuria, G. H. Syed, A. Dixit. Identification of multipotent drugs for COVID-19 therapeutics with the evaluation of their SARS-CoV2 inhibitory activity, ComputStructBiotechnol J. 19 (2021) 1998-2017.https://doi.org/10.1016/j.csbj.2021.04.014.
[4] B. Kumudhaveni, S. Kathirvel, S. D. Muthu, A. Jeradsuresh, R. Radha, Potential drug candidates for treatment of Covid-19, IJPSR.11 (2020) 4087 – 4094. https://doi.org/10.13040/IJPSR.0975-8232.
[5] S. S. Mohanty, C. R. Sahoo, R. N. Padhy, Targeting some enzymes with repurposing approved pharmaceutical drugs for expeditious antiviral approaches against newer strains of COVID-19, AAPS PharmSciTech. 22 (2021) 214.https://doi.org/10.1208/s12249-021-02089-5.
[6] V. Parvathaneni, V. Gupta, Utilizing drug repurposing against COVID-19 - Efficacy, limitations, and challenges, Life Sci. 259 (2020) 118275.https://doi.org/10.1016/j.lfs.2020.118275.
[7] A.Bartoli, F. Gabrielli, T. Alicandro, F. Nascimbeni, P. Andreone, COVID-19 treatment options: A difficult journey between failed attempts and experimental drugs, IEM. 16 (2021) 281–308. https://doi.org/10.1007/s11739-020-02569-9.

[8] S. Bimonte, A. Crispo, A. Amore, E. Celentano, A. Cuomo, M. Cascella, Potential antiviral drugs for SARS-Cov-2 treatment: Preclinical findings and ongoingclinical research. In vivo.34 (2020) 1597–1602. https://doi.org/10.21873/invivo.11949.

[9] M. Malani, P. Salunke, S. Kulkarni, G. K. Jain, A. Sheikh, P. Kesharwani, J. Nirmal, Repurposing pharmaceutical excipients as an antiviral agent against SARS-CoV-2. J BiomaterSciPolym Ed., 33 (2022) 110–136. https://doi.org/10.1080/09205063.2021.1975020.

[10] R. J. Geraghty, M. T. Aliota, L. F. Bonnac, Broad-Spectrum antiviral strategies and nucleoside Analogues, Viruses, 13 (2021) 667. https://doi.org/10.3390/v13040667.

[11] D. L. McKee, A. Sternberg, U. Stange, S. Laufer, C. Naujokat, Candidate drugs against SARS-CoV-2 and COVID-19, Pharmacol. Res. *157* (2020) 104859-104870. https://doi.org/10.1016/j.phrs.2020.104859.

[12] T. Felicett, M. C. Pismataro, V. Cecchetti, O. Tabarrini, S. Massari. Triazolopyrimidine Nuclei: Privileged scaffolds for developing antiviral agents with a proper pharmacokinetic profile. Curr Med Chem. 29 (2022) 1379-1407. https://doi.org/10.2174/0929867328666210526120534.

[13] A. Karthic, V. Kesarwani, R. K. Singh, P. K. Yadav, N. Chaturvedi, P. Chauhan, B. S. Yadav, S. K. Kushwaha. Computational analysis reveals monomethylatedtriazolopyrimidine as a novel inhibitor of SARS-CoV-2 RNA-Dependent RNA Polymerase (RdRp), Molecules. 27(2022) 801.https://doi.org/10.3390/molecules27030801

[14] M. C. Pismataro, T. Felicetti, C. Bertagnin, M. G. Nizi, A. Bonomini, M. L. Barreca, V. Cecchetti, D. Jochmans, S. De Jonghe, J. Neyts, A. Loregian, O. Tabarrini, S. Massari, 1,2,4-Triazolo[1,5-*a*]pyrimidines: Efficient one-step synthesis and functionalization as influenza polymerase PA-PB1 interaction disruptors, Eur J Med Chem. 221 (2021) 113494. https://doi.org/10.1016/j.ejmech.2021.113494.

[15] P. K. Singh, S. Choudhary, A. Kashyap, H. Verma, S. Kapil, M. Kumar, M. Arora, O. Silakari, An exhaustive compilation on chemistry of triazolopyrimidine: A journey through decades, Bioorg Chem. 88 (2019) 102919. https://doi.org/10.1016/j.bioorg.2019.102919.

[16] K. Oukoloff, J. Kovalevich, A. S. Cornec, Y. Yao, Z. A. Owyang, M. James, J. Q. Trojanowski, V. M. Lee, A. B. Smith, 3rd, K. R. Brunden, C. Ballatore, Design, synthesis and evaluation of photoactivatable derivatives of microtubule (MT)-active [1,2,4]triazolo[1,5-*a*]pyrimidines, Bioorg Med ChemLett. 28 (2018) 2180–2183. https://doi.org/10.1016/j.bmcl.2018.05.010.

[17] D. F. A. Lancois, J. É. G. Guillemont, P. J. B. Raboisson, D. A. E. Roymans, B. Rogovoy, V. Bichko, D. Y. R. Lardeau, A. B. Michaut, The antiviral pyrazolos of RSV and triazolopyrimidine compound. Patent (2016)WO2016174079A1.

[18] D. F. A. Lancois, J. É. G. Guillemont, P. J. B. Raboisson, D. A. E. Roymans, P. Rigaux, A. B. Michaut, G. J. M. Mercey, Pyrazolopyrimidines having activity against the respiratory syncytial virus RSV, (2019) Patent WO/2019/106004.

[19] G. H. Elgemeie, A. M. Salah, N. S. Abbas, H. A. Hussein, R. A. Mohamed, Pyrimidine non-nucleoside analogs: A direct synthesis of a novel class of N-substituted amino and *N*-sulfonamide derivatives of pyrimidines,Nucleosides Nucleotides. 36 (2017) 213-223. https://doi.org/10.1080/15257770.2016.1257808.

[20] G. H. Elgemeie, A. M. Salah, R. A. Mohamed,P. G. Jones, Crystal structure of (*E*)-2-amino-4-methylsulfanyl-6-oxo-1-{[(thiophen-2-yl)methylidene]amino}-1,6-dihydro-pyrimidine-5-carbonitrile, Acta Crystallogr E Crystallogr Commun. 71 (2015) 1319–1321. https://doi.org/10.1107/S205698901501885X.

[21] G. H. Elgemeie, R. A. Mohamed, H. A. Hussein, P.G. Jones, Crystal structure of *N*-(2-amino-5-cyano-4-methylsulfanyl-6-oxo-1,6-dihydropyrimidin-1-yl)-4-bromobenzene-sulfonamide dimethylformamidemonosolvate, Acta Crystallogr E Crystallogr Commun. 71 (2015) 1322–1324. https://doi.org/10.1107/S2056989015018903.

[22] G. H. Elgemeie, R. A. Mohamed, Microwave chemistry: Synthesis of purine and pyrimidine nucleosides using microwave radiation, J. Carbohydr. Chem. 38(2019) 1-47. https://doi.org/10.1080/07328303.2018.1543430.

[23] G. H. Elgemeie, A. M. Salah, N. S. Abbas, H. A. Hussein, R. A. Mohamed, Nucleic acid components and their analogs: Design and synthesis of novel cytosine thioglycosideanalogs, Nucleosides Nucleotides.36 (2017) 139-150. https://doi.org/10.1080/15257770.2016.1231318.

[24] G. H. Elgemeie, A. B. Farag, Design, Synthesis, and in Vitro anti-Hepatocellular Carcinoma of Novel Thymine ThioglycosideAnalogs as New Antimetabolic Agents.Nucleosides Nucleotides.36 (2017) 328–342.https://doi.org/10.1080/15257770.2017.1287377.

[25] G. H. Elgemeie, S. A. Alkhursani, R. A. Mohamed, New synthetic strategies for acyclic and cyclic pyrimidinethione nucleosides and their analogues, Nucleosides Nucleotides. 38 (2019) 12–87.https://doi.org/10.1080/15257770.2018.1498511.

[26] S. Scala , N. Akhmed, U. S. Rao, K. Paull, L. B. Lan, B. Dickstein, J. S. Lee, G. H. Elgemeie, W. D. Stein, S. E. Bates, P-Glycoprotein Substrates and Antagonists Cluster into Two Distinct Groups, Mol. Pharmacol. 51 (1997) 1024–1033.https://doi.org/10.1124/mol.51.6.1024.

[27] G. H. Elgemeie, E. M. Mahdy, M. A. Elgawish, M. M. Ahmed, W. G. Shousha, M. E. Eldin, A new class of antimetabolites: pyridine thioglycosides as potential anticancer agents, Z Naturforsch C J Biosci. 65(2010) 577–587. https://doi.org/10.1515/znc-2010-9-1008.

[28] G. H. Elgemeie, R. A. Mohamed-Ezzat, Chapter 6 - Synthetic strategies for purine nucleoside analogs, Editor(s): G. H. Elgemeie, R. A. Mohamed-Ezzat, New Strategies targeting cancer metabolism, Elsevier, 2022, Pages 221-301, ISBN 9780128217832, https://doi.org/10.1016/B978-0-12-821783-2.00002-9.

[29] G. H. Elgemeie, R. A. Mohamed-Ezzat, Chapter 7 - Synthetic strategies for pyrimidine nucleoside analogs, Editor(s): G. H. Elgemeie, R. A. Mohamed-Ezzat, New strategies targeting cancer metabolism, Elsevier, 2022, Pages 303-392, ISBN 9780128217832, https://doi.org/10.1016/B978-0-12-821783-2.00010-8.

[30] M. A. Abu-Zaied, G. H. Elgemeie, N. M. Mahmoud, Anti-Covid-19 drug analogues: Synthesis of novel Pyrimidine thioglycosides as antiviral agents against SARS-COV-2 and avian influenza H5N1 viruses, ACS Omega. 6 (2021) 16890-16904. https://doi.org/10.1021/acsomega.1c01501.

[31] G. H. Elgemeie, R. A. Mohamed-Ezzat, Chapter 10 - Synthetic strategies for antimetabolite analogs in our laboratory, Editor(s): G. H. Elgemeie, R. A. Mohamed-Ezzat, New strategies targeting cancer metabolism, Elsevier, 2022, pp. 547-611, ISBN 9780128217832, https://doi.org/10.1016/B978-0-12-821783-2.00008-X.

[32] G. H. Elgemeie, S. M. Mahdy, M. A. Elgawish, M. M. Ahmed, W.G. Shousha, M. E. Eldin. A new class of antimetabolites: Pyridine thioglycosides as potential anticancer agents, Z Naturforsch C J Biosci. 65 (2010) 577-587. https://doi.org/10.1515/znc-2010-9-1008.

[33] G. H. Elgemeie, R. A. Mohamed-Ezzat, Chapter 1 - Medicinal chemistry of anticancer agents, Editor(s): G. H. Elgemeie, R. A. Mohamed-Ezzat, New strategies targeting cancer metabolism, Elsevier, 2022, pp. 1-33, ISBN 9780128217832, https://doi.org/10.1016/B978-0-12-821783-2.00004-2.

[34] G. H. Elgemeie, R. A. Mohamed-Ezzat, Chapter 3 - Purine-based anticancer drugs, Editor(s): G. H. Elgemeie, R. A. Mohamed-Ezzat, New strategies targeting cancer metabolism, Elsevier, 2022, pp. 69-105, ISBN 9780128217832, https://doi.org/10.1016/B978-0-12-821783-2.00005-4.

[35] G. H. Elgemeie, R. A. Mohamed-Ezzat, Chapter 4 - Pyrimidine-based anticancer drugs, Editor(s): G. H. Elgemeie, R. A. Mohamed-Ezzat, New Strategies Targeting Cancer Metabolism, Elsevier, 2022, pp. 107-142, ISBN 9780128217832, https://doi.org/10.1016/B978-0-12-821783-2.00006-6.

[36] G. H. Elgemeie, R. A. Mohamed, Application of dimethyl *N*-cyanodithioiminocarbonate in synthesis of fused heterocycles and in biological chemistry, Heterocycl. Commun. 20 (2014) 313-331.

[37] G. H. Elgemeie, R. A. Mohamed, Recent trends in synthesis of five- and six-Membered heterocyclesusing dimethyl *N*-cyanodithioiminocarbonate, Heterocycl. Commun. 20 (2014) 257-269.

[38] R. A. Mohamed-Ezzat,G. H. Elgemeie, P. G. Jones.Crystal structures of (E)-2-Amino-4-methylsulfanyl-6-oxo-1-(1-phenylethylidene-amino)-1,6-dihydropyrimidine-5-carbonitrile and (E)-2-Amino-4-methylsulfanyl-6-oxo-1-[1-(pyridin-2-yl)ethylideneamino]-1,6-dihydro-pyrimidine-5-carbonitrile.ActaCrystallogr E CrystallogrCommun. 77 (2021) 547-550.

[39] G. W. Rewcastle, Chapter 8.02 - Pyrimidines and their Benzo Derivatives, Editor(s): A. R. Katritzky, C. A. Ramsden, E. F.V. Scriven, R. J. K. Taylor, Comprehensive Heterocyclic Chemistry III, Elsevier, 2008, pp. 117-272, ISBN 9780080449920, https://doi.org/10.1016/B978-008044992-0.00702-1. http://dtp.nci.nih.gov.

[40] M. R. Boyd, in: B.A. Teicher (Ed.), Cancer Drug Discovery and Development, 2, Humana Press, USA, 1997, pp. 23-43.

[41] A. Monks, D. Scudiero, P. Skehan, R. Shoemaker, K. Paull, D. Vistica, C. Hose, J. Langley, P. Cronise, A. Vaigro-Wolff, Feasibility of a high-flux anticancer drug screen using a diverse panel of cultured human tumor cell lines. Journal of the National Cancer Institute. 83 (1991) 757–766. https://doi.org/10.1093/jnci/83.11.757.

[42] M. R. Boyd, K. D. Paull, Some practical considerations and applications of thenational cancer institute in vitro anticancer drug discovery screen, Drug Dev. Res. 34 (1995) 91-109. https://doi.org/10.1002/ddr.430340203.

[43] R. H. Shoemaker, The NCI60 human tumor cell line anticancer drug screen, Nat. Rev. Cancer. 6 (2006) 813-823. https://doi.org/10.1038/nrc1951.